

# Multi-controlled single-qubit unitary gates based on the quantum Fourier transform

Vladimir V. Arsoski<sup>1,\*</sup>

<sup>1</sup>*School of Electrical Engineering, University of Belgrade,*

*P.O. Box 35-54, 11120 Belgrade, Serbia*

(Dated: August 5, 2024)

Multi-controlled (MC) special unitary (U) gates are widely used in quantum algorithms and circuits. Few state-of-the-art decompositions of MCU gates use non-elementary  $C - R_x$  and  $C - U^{1/2^{m-1}}$  gates resulting in a linear function for the depths of an implemented circuit on the number of these gates. Our approach is based on two generalizations of the multi-controlled X (MCX) gate that uses the quantum Fourier transform (QFT) comprised of Hadamard and controlled-phase gates. For the native gate set used in a genuine quantum computer, the decomposition of the controlled-phase gate is twice as less complex as  $C - R_x$ , which can result in an approximately double advantage of circuits derived from the QFT. The first generalization is based on altering the controlled gates acting on the target qubit. These gates are the most complex and are also used in the state-of-the-art circuits. Our circuit uses half the number of elementary gates compared to the most efficient one, potentially resulting in a smaller error. However, the advantage in time complexity is not twofold, as it was in MCX gates. The second generalization relies on the ZYZ decomposition and uses only one QFT-based circuit to implement the two multi-controlled X gates needed for the decomposition. Since the complexities of this circuit are approximately equal to the QFT-based MCX, our MCU implementation is more advanced than any known existing. The supremacy over the best-known optimized algorithm will be demonstrated by comparing transpiled circuits assembled for execution in a genuine quantum device.

PACS numbers: 03G12, 81P68

Keywords: Quantum computing, Quantum algorithms, Multi-controlled gates, Quantum Fourier transform

## I. INTRODUCTION

Current quantum devices are constrained by the number of qubits available and the noise introduced during the execution of nonideal quantum operations employing the native gates used for computation in a genuine quantum device. The hardware of these Noisy Intermediate-Scale Quantum devices (NISQ) [1] is constantly improving by increasing the number of qubits and fidelity of the native gates used in a particular quantum computing architecture. However, the efficiency in performing quantum computation can be improved by optimizing software that defines a quantum circuit implementation. It can be achieved by more efficient error mitigation [2], quantum state preparation [3–5], and decomposition of unitary gates into scalable quantum circuits in the basis set of elementary gates [6–9]. The decomposition of a circuit is usually not unique. Therefore, different optimization techniques can be used to minimize the circuit’s depth and (or) the number of elementary gates used [10–12].

The first algorithm for decomposing multi-controlled  $U(2)$  gates, which doesn’t use auxiliary qubits, was proposed in Ref. [6]. It exhibits a quadratic increase in the circuit depth and number of elementary gates with the number of control qubits. The authors showed that implemented circuits can be efficiently reduced by removing some gates at the price of phase relativization, using ancilla qubits, and approximating gates up to the target error  $\epsilon$ . The advantages of using relative-phase Toffoli gates to obtain linear depths of  $n$ -qubit MCX gates were first recognized in Ref. [13]. The effectiveness of this approach is demonstrated theoretically [14] and experimentally [15]. To correct phases, an additional  $(C - R_x)$ -based circuit is introduced in Ref. [16] that approximately doubles the complexity of the previously simplified circuit. Different approximations are used to reduce the number of elementary gates in this circuit [17, 18]. As for all other cases, using auxiliary qubits lowers the circuit depth [19, 20].

## II. RELATED WORK

Our approach is based on the QFT and inspired by basic quantum arithmetic [21]. One may show that simple QFT-based increment/decrement by one can be used to implement

---

\* vladimir.arsoski@etf.bg.ac.rs

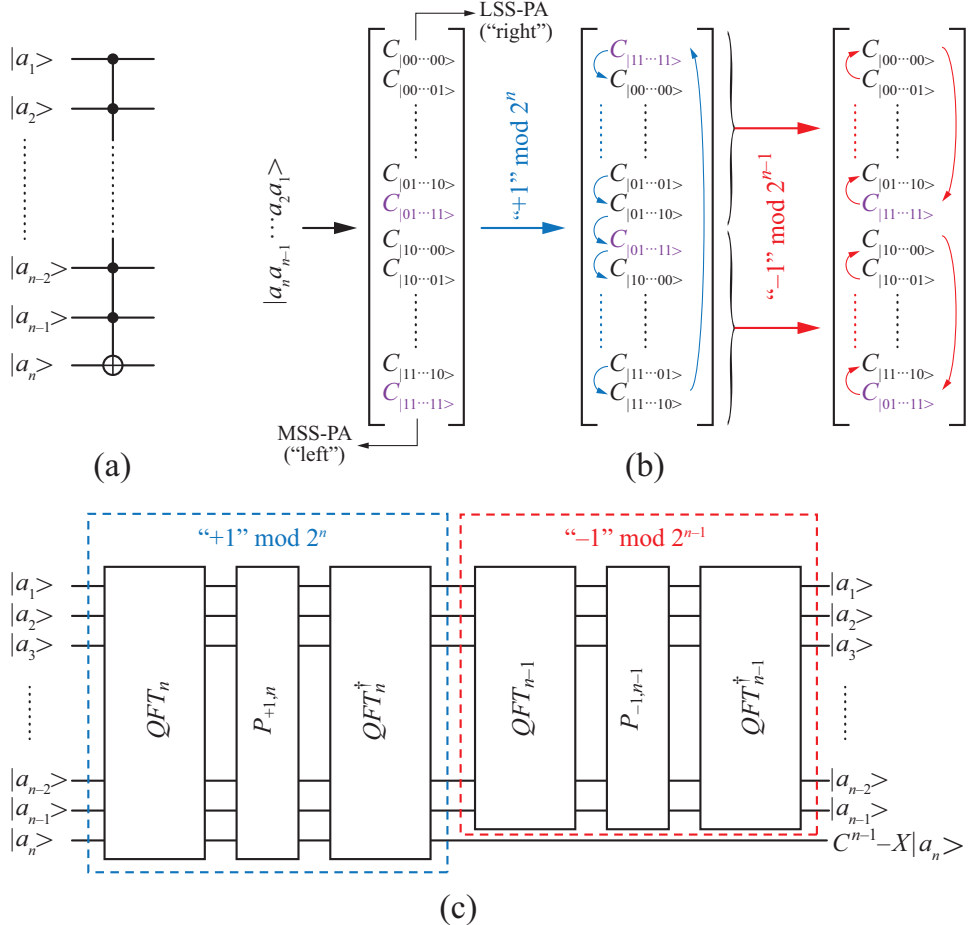


FIG. 1. (a) Schematic view of  $n$ -qubit multi-controlled  $X$  gate, (b) illustration of increment/decrements action on the state vector, and (c) implementations block diagram using QFTs and phase gates. In panel (b), MSS-PA (most significant state's probability amplitude) in classical computing ordering is on the left, while LSS-PA (least significant state's probability amplitude) is on the right.

multi-controlled X gates. The equivalence between the QFT-based MCX and the standard one is rigorously proved theoretically [22]. However, a fairly simple explanation can give us an insight into the principles of the proposed implementation. Multi-controlled gate, shown in Fig. 1(a), executes  $X$  operation on the highest  $n^{\text{th}}$  qubit based on the state of  $(n-1)$  lower qubits. A pure  $n$ -qubit state  $|a\rangle = |a_n a_{n-1} \cdots a_2 a_1\rangle$  is represented by a  $2^n$  dimensional state vector in Hilbert space. The set of orthonormal basis states  $\{|000 \cdots 000\rangle, |000 \cdots 001\rangle, \dots, |111 \cdots 110\rangle, |111 \cdots 111\rangle\} = \{|0\rangle, |1\rangle, \dots, |2^n-2\rangle, |2^n-1\rangle\}$  span this linear vector space. Each term in the state vector  $C_{|k\rangle}$  (where  $k \in \{0, 2^n-1\}$ ) is

the probability amplitude (weight) of the corresponding basis state. An application of MCX on a  $n$ -qubit system results in the swap between  $C_{|011\dots111\rangle}$  and  $C_{|111\dots111\rangle}$  weights.

Arithmetic operations performed on a  $n$ -qubit state are congruent modulo  $2^n$ . To implement MCX, we initially increment a qubit state by one. The weight of  $|k\rangle$  state becomes the weight of  $|(k + 1) \bmod 2^n\rangle$ . Thus, all weights are circularly shifted by one, as shown in Fig. 1(b). Performed on a classical register that stores bits, this operation is known as the circular shift to the left. To restore values of control qubits, we have to execute decrements by one on the quantum register comprised of lower  $(n - 1)$  qubits. Thus, we perform the quantum circular shift to the right in the basis subsets  $|0b_{n-1}\dots b_m\dots b_1\rangle$  and  $|1b_{n-1}\dots b_m\dots b_1\rangle$  where  $b_m \in \{0, 1\}$ , as displayed in Fig. 1(b). As a result, we swapped target states' probability amplitudes thereby implementing the MCX operation. A block schematic of  $n$ -qubit MCX implementation is shown in Fig. 1(c).

A standard QFT implementation uses phase gates:

$$R_m = P\left(\frac{\pi}{2^{m-1}}\right) = \begin{bmatrix} 1 & 0 \\ 0 & e^{i\frac{2\pi}{2^m}} \end{bmatrix} = \begin{bmatrix} 1^{1/2^{m-1}} & 0 \\ 0 & (e^{i\pi})^{1/2^{m-1}} \end{bmatrix} = Z^{1/2^{m-1}}. \quad (1)$$

Increments and decrements by one can be executed using a QFT-based adder [21]. This method computes QFT on the first addend and uses  $R_m$  gates to evolve it into QFT of the sum based on the second addend. Then, the inverse of the QFT ( $\text{QFT}^\dagger$ ) returns the result to the computational basis. Thus, the increment by one is executed by  $\text{QFT}_n^\dagger P_{+1,n} \text{QFT}_n |a\rangle = |a + 1 \bmod 2^n\rangle = C^{n-1} X |a_n\rangle \otimes |a_{n_c} + 1 \bmod 2^{n-1}\rangle$ , where  $P_{+1,n} = Z^{1/2^{n-1}} \otimes Z^{1/2^{n-2}} \otimes \dots \otimes Z^{1/2} \otimes Z$  and  $|a_{n_c}\rangle = |a_{n-1}a_{n-2}\dots a_2a_1\rangle$  is the register comprised of lower  $(n - 1)$  control qubits. This part of the schematic is framed by a blue dashed line and labeled by “ $+1$  mod  $2^n$ ” in Fig. 1(c). To restore control qubits to the initial value, we execute decrement by one  $I_{2\times 2} \otimes \text{QFT}_{n-1}^\dagger P_{-1,n-1} \text{QFT}_{n-1} (C^{n-1} X |a_n\rangle \otimes |a_{n_c} + 1 \bmod 2^{n-1}\rangle) = C^{n-1} X |a_n\rangle \otimes |a_{n_c}\rangle$ , where  $P_{-1,n-1} = Z^{1/2^{n-2}\dagger} \otimes \dots \otimes Z^{1/2\dagger} \otimes Z^\dagger$  and  $I_{2\times 2}$  is the identity  $2 \times 2$  matrix. This part of the circuit is framed by a red dashed line and labeled by “ $-1$  mod  $2^{n-1}$ ” in Fig. 1(c).

The decomposition of the circuit from Fig. 1(c) for 5 qubits is shown in Fig. 2. To estimate the time complexity of the circuit, gates that can execute simultaneously are assembled in a single time slot bounded by a vertical dashed gray line in Fig. 2. Control qubits are  $|a_1\rangle - |a_4\rangle$ , and the target is  $|a_5\rangle$ . Let us consider the “ $+1$  mod  $2^5$ ” part of the circuit and find the value at the target qubit in the more general case of the  $n$ -qubit MCX. Controlled

phase gates ( $C - R_m = C - Z^{1/2^{m-1}}$ ), which act on the target qubit, are represented by gray circles. There are  $(2n-1)$  of these gates. The first  $(n-1)$  gates (to the left) are conditioned on the qubits of the control register  $|a_c\rangle = |a_{n-1}\cdots a_1\rangle$ , the central gate is unconditional, and the last  $(n-1)$  gates are controlled by  $|a_c + 1 \bmod 2^{n-1}\rangle = |a'_{n-1}\cdots a'_1\rangle$ . In a simplified notation, the action of these gates on a target wireline is

$$\begin{aligned}
& \left( Z^{\frac{a'_{n-1}}{2^1}} Z^{\frac{a'_{n-2}}{2^2}} \cdots Z^{\frac{a'_1}{2^{n-1}}} \right) Z^{\frac{1}{2^{n-1}}} \left( Z^{\frac{a_1}{2^{n-1}}} Z^{\frac{a_2}{2^{n-2}}} \cdots Z^{\frac{a_{n-1}}{2}} \right) \\
& = \left( Z^{\frac{2^0 a'_1 + 2^1 a'_2 + \cdots + 2^{n-3} a'_{n-2} + 2^{n-2} a'_{n-1}}{2^{n-1}}} \right)^\dagger Z^{\frac{1+2^0 a_1 + 2^1 a_2 + \cdots + 2^{n-3} a_{n-2} + 2^{n-2} a_{n-1}}{2^{n-1}}} \\
& = Z^{\frac{1+a_c \bmod 2^{n-1}}{2^{n-1}}} Z^{\frac{1+a_c}{2^{n-1}}}.
\end{aligned} \tag{2}$$

This expression is the identity in all cases except for  $a_1 = a_2 = \cdots = a_{n-2} = a_{n-1} = 1$  when  $(1 + a_c \bmod 2^{n-1}) = 0$  and  $1 + a_c = 2^{n-1}$  so the expression is  $Z$ . Since  $HZH = X$ , when the controls are uncomputed by “ $-1$ ”  $\bmod 2^{n-1}$ , the overall circuit executes MCX.

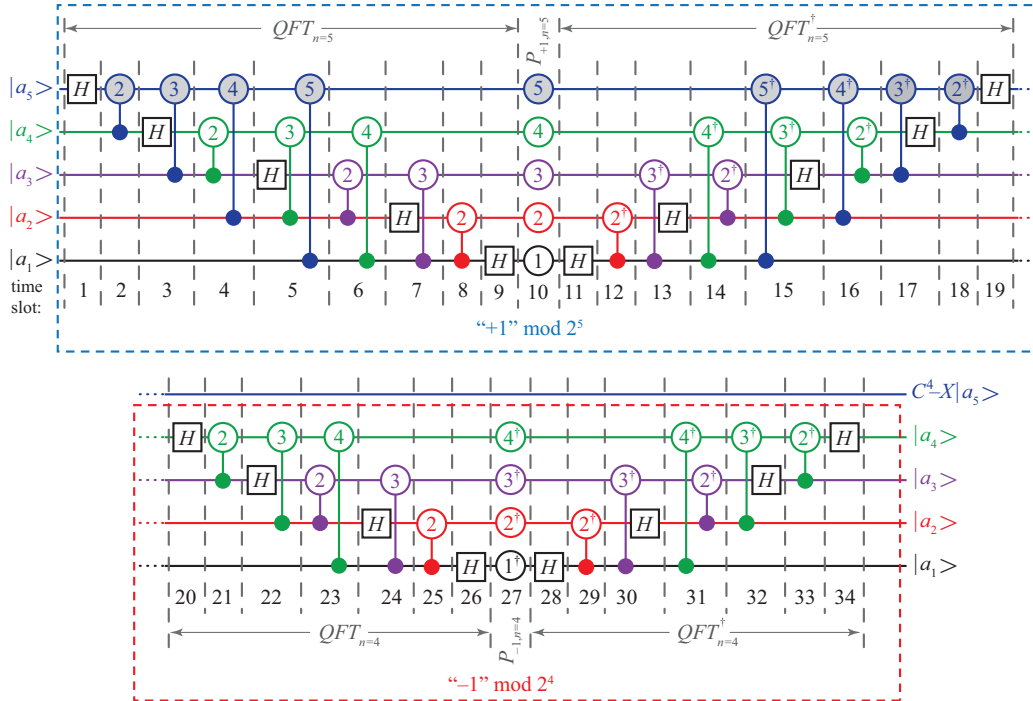


FIG. 2. The decomposition of MCX using non-elementary  $H$ ,  $R_m$  and  $C - R_m$  gates. The circle indicates phase gate  $R_m$  with index  $m$  inscribed. Gates are divided into time slots by vertical gray dashed lines, where the index of the time slot is denoted at the bottom.

On the first wireline there is  $HR_1H = HZH = X$  (slots 9 to 11 in Fig. 2) and  $HR_1^\dagger H =$

$HZ^\dagger H = X^\dagger = X$  (slots 26 to 28 in Fig. 2). The phase gates controlled by the first qubit are applied at the beginning of QFT and end of  $\text{QFT}^\dagger$ . These gates can merge using the equivalence shown in Fig. 3. Thus, there is no need to implement  $P$  separately. Moreover, the QFT in “ $+1$  mod  $2^n$ ” and the  $\text{QFT}^\dagger$  in “ $-1$  mod  $2^{n-1}$ ” will also have a set of  $C - R_m$  gates less. A detailed explanation of implementation, optimization, calculation of circuit complexities, and proof of principle is elaborated in Ref. [22].

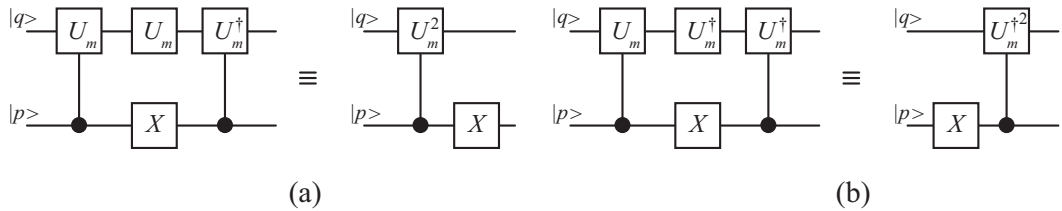


FIG. 3. The identities for merging gates in (a) “ $+1$  mod  $2^n$ ” and (b) “ $-1$  mod  $2^{n-1}$ ”.  $U_m$  is a single qubit unitary gate. For  $U = R_m = Z^{1/2^{m-1}}$ ,  $U^2 = R_{m-1} = Z^{1/2^{m-2}}$ .

### III. MULTI-CONTROLLED U(2) GATES

The aim is to generalize the MCX circuit to a multi-controlled single-qubit unitary gate (MCU). We will explore implementations in two distinct quantum computer architectures to find the lower and upper bounds for the time and space complexities. The most favorable architecture supports interaction between arbitrary pairs of qubits, implying that the system is fully connected (FC). Implementation in this architecture is the least complex, setting the lower complexity bounds. The most restricted is the linear one allowing interactions only between nearest-neighbours (LNN). Using this architecture demands swapping many qubits to perform two-qubit gates, and additional SWAP gates increase the time and space complexities. We use two strategies to generalize the circuit. The first is based on modifying the QFT-based MCX gate, while the second uses extended optimized MCX gates and well-known  $ZYZ$  (that is,  $ABC$ ) decomposition [6].

It is straightforward to conclude from Eq. 2 that by substituting  $R_m = Z^{1/2^{m-1}}$  with  $U_m = U^{1/2^{m-1}}$  on the target qubit and omitting  $H$  gates, the circuit implements a multi-controlled special unitary  $U$  gate. Schematic views of 5-qubit MCUs in the FC and LNN architecture are given in Figs. 4(a) and (b), respectively. If  $U$  is not a special unitary, then

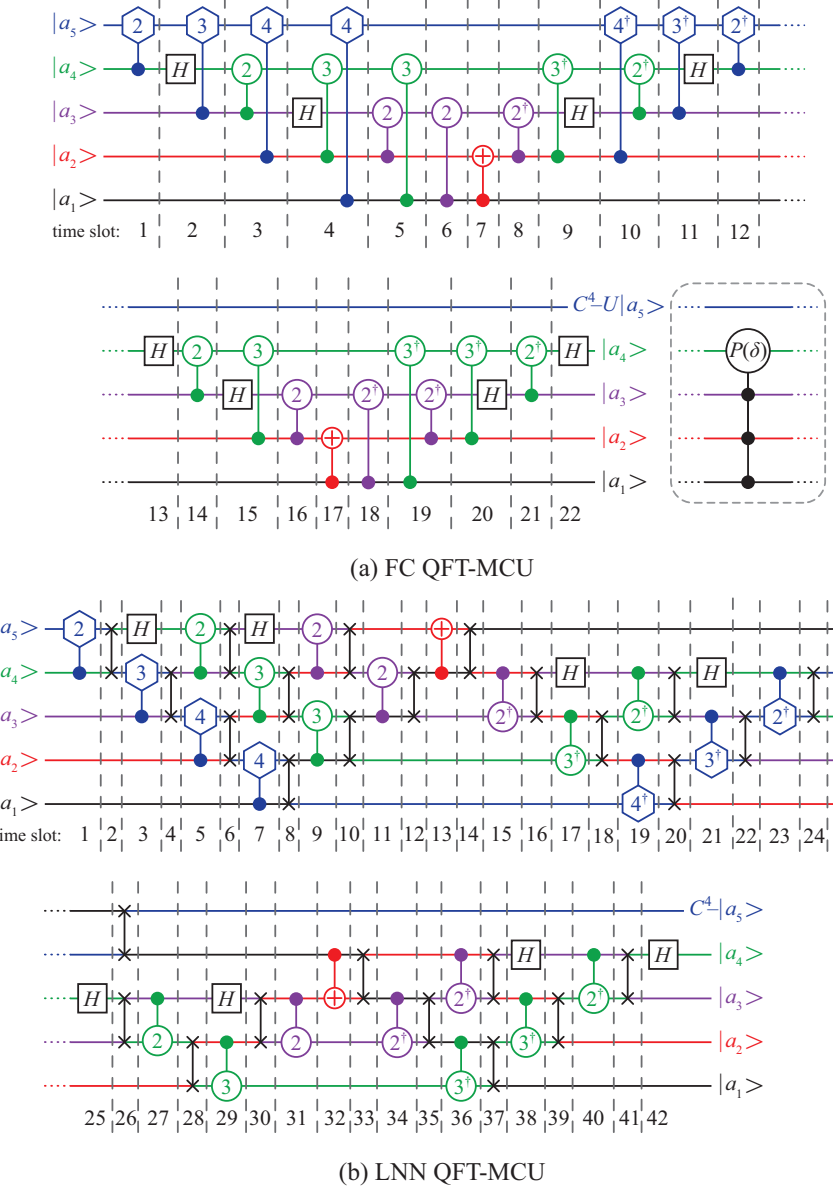


FIG. 4. A schematic of five-qubit MCU implementations based on QFT-MCX modification in the (a) fully connected (FC) and (b) linear nearest-neighbor (LNN) quantum computer architecture. Circles denote phase gates  $R_m = Z^{1/2^{m-1}}$  while hexagons represent unitary  $U_m = U^{1/2^{m-1}}$  gates, with the value  $m$  inscribed into gate symbols. To estimate the time complexity, gates that can execute simultaneously are divided into time slots.

$U(2) = e^{i\delta} SU(2)$ , where  $\delta$  is a real valued. In this case, the circuit will introduce a phase shift to probability amplitudes of the basis states  $|b_n \cdots b_1\rangle$ . To implement an arbitrary multi-controlled  $U(2) \notin SU(2)$ , we separately implement multi-controlled  $SU(2)$  and the controlled phase circuit  $C_1 C_2 \cdots C_{n-2} - P_{n-1}(\delta)$  that adds the phase factor  $e^{i\delta}$ , as shown in

the insert in Fig. 4(a). However, the  $P(\delta)$  gate is not  $SU(2)$ . Therefore,  $C - P$  will exhibit the same phase relativization issue, so it should be implemented using an alternative circuit.

One may show that FC QFT-MCU executes in  $(8n - 18)$  time slots. It comprises of  $4(n - 3)$  single-qubit Hadamards,  $2(n - 1)(n - 3)$  controlled phase gates, two  $C$ -NOTs and  $(2n - 3)$   $C - U^{1/2^{m-1}}$  gates. An approximate QFT (AQFT) may provide greater accuracy than a full QFT in the presence of decoherence [23]. Controlled phases  $R_m$  with  $m \leq \lceil \log_2 n \rceil$  are used in AQFT. Therefore, the number of controlled gates reduces to  $2(\lceil \log_2 n \rceil - 1)(2n - 3 - \lceil \log_2 n \rceil)$  and  $2(\lceil \log_2 n \rceil - 1)$ ,  $C - R_m$  and  $C - U_m$  gates, respectively.

Using the systematic approach for swapping qubits in finite-neighbor quantum architectures [24], one may find that LNN QFT-MCU needs  $(8n - 20)$  time slots with  $(2n^2 - 6n + 6)$  SWAP gates. Therefore, LNN uses approximately twice the number of time slots and gates as FC QFT-MCU, thus setting the upper bound for the time and space complexities.

Actual circuit depth and the number of gates implemented depend on the native gate set (NGS) of the quantum device used in the calculation. The decomposition of a non-elementary gate uses a few elementary gates executed in a certain number of time slices. This number of time slices defines the circuit depth. One should note that some elementary gates can be executed in parallel and some cancel out, as explained in Ref. [22] for the selected NGS. Elementary gates that comprise the NGS have a high but finite fidelity. Also, current quantum devices are prone to noise and decoherence. Therefore, low-depth circuits using fewer elementary gates are less prone to errors.

The advantage of using QFT to implement MCU relies on the efficient decomposition of controlled phase gates. The state-of-the-art linear-depth decomposition (LDD) of MCU [16, 18] use  $C - X^{1/2^{m-1}}$  and  $C - U_m = C - U^{1/2^{m-1}}$  gates. A recent paper showed that the circuit can be simplified by omitting gates with  $m > \lceil \log_2 n \rceil$  [18] similar to the approximate QFT approach. We should note that the QFT-based MCU circuit uses approximately the same number of non-elementary gates as the state-of-the-art one. However, the decomposition of  $C - R_m$  in the NGS of superconducting hardware is twice as less complex as  $C - X^{1/2^{m-1}}$  leading to approximately double the advantage of the QFT-based approach when implementing MCX [22]. In the case of a random special unitary gate, the depth of the MCU circuit is predominantly determined by the complexity of the  $C - U_m$  decomposition. Since our approach uses the same sequence of gates on the target qubit wireline, the difference in the depths will be smaller than in the case of MCX. However, the number of

elementary gates in our approach is still twice as small.

The main problem in using the  $C - R_x$  [16, 18] and QFT-based MCU decomposition is related to the complexity and precision of  $C - U_m$  implementation. Moreover, a similar issue exists for  $C - X^{1/2^{m-1}}$  and  $C - R_m$ , but it is less pronounced in the QFT-based approach since the latter has a simple decomposition.

A more effective circuit can be obtained using the  $ZYZ$  decomposition. For a single-qubit unitary matrix expressed as  $U = e^{i\delta} R_z(\alpha) R_y(\theta) R_z(\beta)$ , there is a set of matrices  $A = R_z(\alpha) R_y(\theta/2)$ ,  $B = R_y(-\theta/2) R_z(-(\alpha+\beta)/2)$ , and  $C = R_z((\beta-\alpha)/2)$  such that  $ABC = I_{2 \times 2}$  and  $U = e^{i\delta} AXBXC$  [6]. We will explain the functionality of “ $+1$ ” and “ $-1$ ” blocks to make clear how we found an optimal circuit. Using an iterative approach, we show that the “ $+1$ ” mod  $2^n$  circuit

$$\begin{aligned}
QFT_n^\dagger P_{+1,n} QFT_n |a\rangle &= |a + 1 \bmod 2^n\rangle \\
&= (C_1 C_2 \cdots C_{n-2} C_{n-1} - X |a_n\rangle) \otimes |a_{n_c} + 1 \bmod 2^{n-1}\rangle \\
&= (C_1 \cdots C_{n-1} - X |a_n\rangle) \otimes (C_1 \cdots C_{n-2} - X |a_{n-1}\rangle) \otimes |a_{n_c-1} + 1 \bmod 2^{n-2}\rangle \\
&= (C_1 \cdots C_{n-1} - X |a_n\rangle) \otimes \cdots \otimes (C_1 - X |a_2\rangle) \otimes (X |a_1\rangle), \tag{3}
\end{aligned}$$

is equivalent to the stair-wise array of controlled  $X$  gates, and “ $-1$ ” mod  $2^n$  is its inverse (see Fig. 5). To implement two MCX gates needed for  $ABC$ -based MCU, we will use a single QFT-based MCX circuit with “ $-1$ ” mod  $2^n$  instead of  $I_{2 \times 2} \otimes$  (“ $-1$ ” mod  $2^{n-1}$ ), as shown in Fig. 5. Therefore, the complexity of the circuit is approximately equal to the QFT-MCX, where we use only additional  $A$ ,  $B$ , and  $C$  single-qubit gates found by  $ZYZ$  decomposition of  $U \in SU(2)$ . Detailed schematics of QFT-MCU in FC and LNN architectures can be found in Ref. [22]. For general multi-controlled single-qubit  $U(2)$  gate implementation, an additional  $(n-1)$ -qubit controlled phase gate should be used. The same circuit can add the phase in our former and LDD-based implementation.

The QFT-based subcircuits (“ $+1$ ” and “ $-1$ ”) implement two MCX gates and are executed in  $(8n - 12)$  time slots in the FC architecture. There are  $4(n-2)$  Hadamard gates,  $2n(n-2)$  controlled phases, and two  $C - X$  gates. AQFT reduces the number of  $C - R_m$  gates to  $2([\log_2 n] - 1)(2n - 1 - [\log_2 n])$ . At most three time slots are required for executing  $A$ ,  $B$ , and  $C$ . These gates use a total of three  $R_z$  and two  $R_y$  gates. The LNN implementation uses an additional  $(8n - 16)$  time slots with  $2(n-1)^2$  SWAP gates.

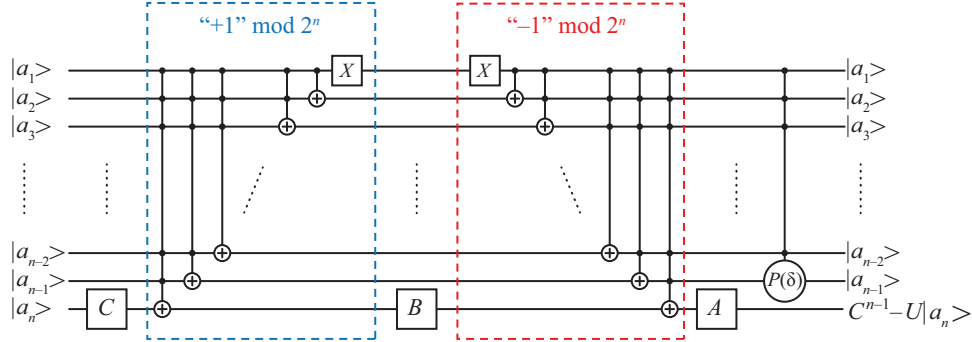


FIG. 5. A schematic of  $n$ -qubit MCUs implementation based on the  $ZYZ$  decomposition and QFT.

#### IV. ANALYTICAL AND NUMERICAL ANALYSIS

To get theoretical bounds for complexities in a genuine quantum computation, we chose the native gate set  $\{C - X, R_z, ID, SX = \sqrt{X}, X\}$ , which is one of a few sets used by superconducting hardware. One may show that  $R_m = \exp(i\frac{\pi}{2^m}) \cdot R_z(\frac{\pi}{2^{m-1}})$ ,  $H = \exp(i\frac{\pi}{4}) \cdot R_z(\frac{\pi}{2})\sqrt{X}R_z(\frac{\pi}{2})$ ,  $R_y = \sqrt{Z}HR_zH\sqrt{Z}^\dagger$ , and  $SWAP_{12} = (C_1 - X_2)(C_2 - X_1)(C_1 - X_2)$  [7]. Hadamard and SWAP use three native gates and three elementary time intervals to execute, while  $R_y$  and  $C - R_m$  use five. Employing parallelization, the depths of  $H$  and  $C - R_m$  gates are effectively reduced to two and four, respectively. Some of the  $R_z$  gates can be executed simultaneously, some will merge, and the one between QFT and  $QFT^\dagger$  will cancel out, as elaborated in Ref. [22]. Merging consecutive  $R_z$  gates,  $A$  and  $B$  comprise 5 elementary gates, and  $C$  uses one  $R_z$  gate. There are two  $SWAP \cdot C - X$  gates in the LNN implementation, where two  $C - X$  gates annihilate in each. In the most general case, the decomposition of a controlled single-qubit unitary gate in the NGS uses 14 elementary gates (two  $C - X$ , four  $\sqrt{X}$ , and the rest are  $R_z$ ) that execute in 13 elementary time intervals. Merging  $R_z$ 's of neighboring  $U_m$  gates, the depth and the number of elementary gates effectively reduce by one (except for the first or the last gate on the target wireline). One should note that the decomposition of some  $C - U$  gates (excluding  $C - X$  or  $C - Z$ , since comprised in the basis gate set of superconducting quantum devices) is less complex, where  $C - R_z$  and  $C - P$  are some of the simplest. In the approximate form of QFT-MCU, we will use  $R_m$  and  $U_m$  with  $m \leq \lceil \log_2 n \rceil$ , which results in a low error [18]. We will derive the lower and upper bounds for the circuit depth and number of elementary gates for a multi-controlled  $SU(2)$  gate. All bounds, expressed as a function of the number of qubits used, are derived using the selected

NGS. We will not use any additional specific optimization available in quantum computing software.

By counting in the NGS, FC-MCU based on MCX modification has the depth  $(34n - 56)$ . The circuit uses  $(6n^2 - 8n - 13)$   $R_z$ ,  $12(n - 2)$   $\sqrt{X}$  or  $\sqrt{X}^\dagger$ , and  $4(n^2 - 3n + 4)$   $C - X$  gates. By approximating the QFT, the number of  $R_z$ ,  $\sqrt{X}$ , and  $C - X$  gates will be reduced by  $6(n^2 - 4n - (\lceil \log_2 n \rceil - 1)(2n - 5 - \lceil \log_2 n \rceil))$ ,  $4(2n - 2 - 2(\lceil \log_2 n \rceil - 1))$ , and  $2(2n(n - 3) - 2(\lceil \log_2 n \rceil - 1)(2n - 2 - \lceil \log_2 n \rceil))$ , respectively. Due to additional SWAP gates used, the depth of the LNN circuit is greater by  $(24n - 64)$  for  $n > 3$ . Also, the number of  $C - X$  gates increases by  $(6n^2 - 18n + 14)$ .

FC-MCU based on the  $ZYZ$  decomposition has the depth  $(32n - 44)$ . It uses  $(6n^2 - 8n - 4)$   $R_z$ ,  $4(n - 1)$   $\sqrt{X}$  or  $\sqrt{X}^\dagger$ , and  $(4n^2 - 6)$   $C - X$  gates. Using AQFT will reduce the number of  $R_z$  and  $C - X$  gates by  $6(n(n - 2) - (\lceil \log_2 n \rceil - 1)(2n - 1 - \lceil \log_2 n \rceil))$  and  $4(n(n - 2) - (\lceil \log_2 n \rceil - 1)(2n - 1 - \lceil \log_2 n \rceil))$ , respectively. Due to additional SWAP gates used, the depth of the LNN circuit is greater by  $(24n - 52)$  for  $n > 3$ , while the number of  $C - X$  gates increases by  $(6n^2 - 12n + 2)$ . Based on the metric provided, we can readily determine the complexities of the phase-adding gate.

We consider the AQFT FC-MCU the lower and LNN-MCU the upper bound on the number of elementary gates and the circuit depth in a genuine quantum computation. Estimated complexities for application on a quantum device are obtained by assembling analyzed circuits using the transpile function built-in Python package Qiskit v.0.42.1 [25]. In doing so, we used optimization level 3. To remove any doubt about bias in our implementation, we used the local simulator to transpile circuits for application on the ‘ibm\_hanoi’ employed in Refs. [16, 18] although it was retired recently. We compare our implementations to the standard Qiskit and the state-of-the-art MCU circuit. The unitary single-qubit gate used in all analyzed MCU circuits was randomly chosen from  $SU(2)$  gates. To get angles  $\alpha$ ,  $\theta$ , and  $\beta$ , we have generated random rational numbers and multiplied them by  $\pi$ . We constrained our choice to exclude trivial gates. The comparison of circuit depths is displayed in Fig. 6.

The default Qiskit implementation performs the worst exhibiting an exponential increase in time complexity with the number of qubits. Circuit depths of either LDD or QFT-based MCUs are linear in the number of qubits. Both LDD and QFT-MCU use  $C - U_m$  gates which have a complex decomposition. It increases the circuit depth compared to MCX implementation. However, LDD uses  $C - R_x$  gates that are more complex than  $C - R_m$

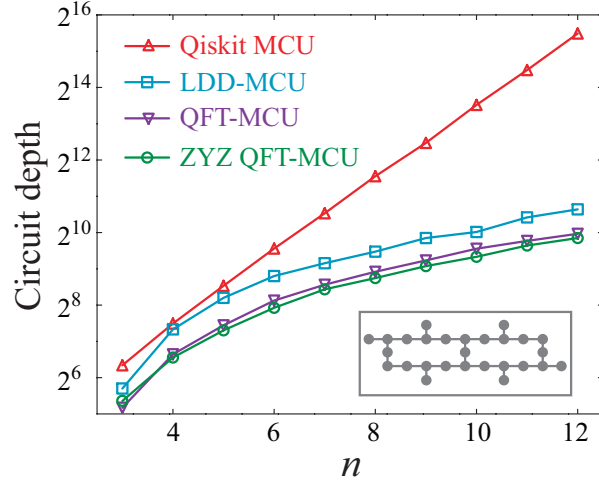


FIG. 6. The dependence of circuit depths on the number of qubits in **default Qiskit** ( $\Delta$ ), **LDD-MCU** from Ref. [16] ( $\square$ ), **QFT-MCU** ( $\nabla$ ), and **ZYZ QFT-MCU** ( $\circ$ ). The layout of the quantum processor is shown in the insert.

comprising QFT-based implementation. Therefore, the circuit depths of LDD-MCU are larger than QFT-MCU although they have a similar construction. Finally, the *ZYZ*-based decomposition of the QFT-MCU is approximately as complex as the MCX circuit, thus exhibiting the least circuit depth of all implementations. Not only does it use the smallest number of elementary gates and have the lowest circuit depth, but it also doesn't employ  $C - U_m$  gates. To implement  $U^{1/2^{m-1}}$  we have to use gates having small angles as the argument if  $m$  is large. A matrix representation of small-angle gates is close to the unity matrix. Therefore, it is debatable if the LDD and the QFT-MCU that use  $U_m$  can be implemented with sufficient precision in a genuine quantum device.

Lastly, let's analyze some additional simplifications beyond current software optimization capabilities. There are control phase gates,  $C_k - R_{m,j}$ , applied to  $|a_k\rangle$  as the control and  $|a_j\rangle$  as the target in both of our implementations. The decomposition of these subcircuits is

$$\begin{aligned}
 & (I_{2 \times 2} \otimes P(\frac{\pi}{2^m}))(C - X)(I_{2 \times 2} \otimes P(-\frac{\pi}{2^m}))(C - X)(P(\frac{\pi}{2^m}) \otimes I_{2 \times 2})(|a_k\rangle \otimes |a_j\rangle) \\
 &= (I_{2 \times 2} \otimes R_z(\frac{\pi}{2^m}))(C - X)(I_{2 \times 2} \otimes R_z(-\frac{\pi}{2^m}))(C - X)(P(\frac{\pi}{2^m}) \otimes I_{2 \times 2})(|a_k\rangle \otimes |a_j\rangle) \\
 &= (C - R_z(\frac{\pi}{2^m}))(P(\frac{\pi}{2^m}) \otimes I_{2 \times 2})(|a_k\rangle \otimes |a_j\rangle),
 \end{aligned} \tag{4}$$

where we used the identity  $P(\gamma)XP(-\gamma) = R_z(\gamma)XR_z(-\gamma)$ . In Ref. [22] we showed that these gates between “+1” and “-1” circuits annihilate. Thus, on each control wireline we

will have  $P(\frac{\pi}{2^m})$  at the beginning (shown in red in Eq. 4), and  $P(-\frac{\pi}{2^m})$  at the end. These gates also cancel out if all lower ( $k-1$ ) control qubits are one (when we have  $P(\frac{\pi}{2^m})XXP(-\frac{\pi}{2^m}) = I_{2 \times 2}$ ), or if they are not (when we have  $P(\frac{\pi}{2^m})P(-\frac{\pi}{2^m}) = I_{2 \times 2}$ ). Therefore, we can omit these phase gates and use  $C - R_z(\pi/2^{m-1})$  instead of  $C - R_m$  simplifying our circuit.

Following the discussion above, we were wondering if LDD-MCU can be simplified. We found that if we insert two consecutive Hadamard gates between  $R_x$  gates from Ref. [16, 18] (where  $HH = I_{2 \times 2}$ ), and using  $HR_x(\gamma)H = R_z(\gamma)$ , all the  $C - R_x(\gamma)$  gates will transform to  $C - R_z(\gamma)$ . Note that on the second wireline, we put two  $H$  gates on each side of  $R_x(\pm\pi)$ 's, and we don't need to add Hadamards on the first wireline. When we perform the transformation described, each control wireline, except the first one, will have one  $H$  gate 'remaining' at the beginning and the end of the  $C - R_z$  sequence. Knowing that  $HR_z(\pi)H = e^{-i\pi/2}HZH = -iX$  and  $HR_z(-\pi)H = e^{i\pi/2}HZH = iX$ , we can replace  $C_1 - R_z(\pi)$  and  $C_1 - R_z(-\pi)$  by two  $C - X$  gates. Thus, the LDD-MCU is reduced to our QFT-MCU based on QFT-MCX modification, which will reduce the number of gates used and the circuit depth by approximately twice.

## V. CONCLUSIONS

In this paper, we have presented two new implementations of multi-controlled unitary (MCU) gates. The first implementation is based on the modification of a multi-controlled X (MCX) gate that uses the quantum Fourier transform (QFT), where the phase gates acting on the target qubit ( $Z^{1/2^{m-1}}$ ) are replaced with the adequate roots of the single-qubit unitary gate ( $U^{1/2^{m-1}}$ ). This is similar to the state-of-the-art LDD circuit but has a lower circuit depth and uses approximately twice as few elementary gates. The main disadvantage of the former two implementations is that they both use  $U^{1/2^{m-1}}$  gates, which are hard to implement with desired precision. The second implementation is based on the  $ZYZ$  decomposition and uses an extended QFT-based MCX circuit to implement the two MCX gates needed for the decomposition. This implementation has lower time and space complexities compared to any existing MCU. Simplification of this circuit can be achieved straightforwardly using an approximation of the QFT or by introducing auxiliary qubits, which was elaborated in our previous work on the MCX. The supremacy of this implementation was demonstrated by analyzing transpiled circuits, where our MCU exhibited a noticeable advantage compared

to the existing state-of-the-art implementation.

Finally, we showed that our circuits can be further simplified by replacing  $C - R_m$  gates with  $C - R_z$ . Moreover, we demonstrated that the state-of-the-art LDD-MCU can be simplified to our QFT-MCU based on QFT-MCX modification, thus significantly reducing the LDD's time and space complexities.

---

- [1] John Preskill, “Quantum Computing in the NISQ era and beyond”, *Quantum* **2**, 79 (2018).
- [2] Youngseok Kim, Andrew Eddins, Sajant Anand, Ken Xuan Wei, Ewout van den Berg, Sami Rosenblatt, Hasan Nayfeh, Yantao Wu, Michael Zaletel, Kristan Temme, and Abhinav Kandala, “Evidence for the utility of quantum computing before fault tolerance,” *Nature* **618**(7965), 500–505 (2023).
- [3] Martin Plesch and Časlav Brukner, “Quantum-state preparation with universal gate decompositions,” *Physical Review A* **83**(3), 032302 (2011).
- [4] Xiao-Ming Zhang, Man-Hong Yung , and Xiao Yuan, “Low-depth quantum state preparation,” *Physical Review Research* **3**(4), 043200 (2021).
- [5] Israel F. Araujo, Daniel K. Park, Francesco Petruccione, and Adenilton J. da Silva, “A divide-and-conquer algorithm for quantum state preparation,” *Scientific reports* **11**(1), 6329 (2021).
- [6] Adriano Barenco, Charles H. Bennett, Richard Cleve, David P. DiVincenzo, Norman Margolus, Peter Shor, Tycho Sleator, John A. Smolin, and Harald Weinfurter, “Elementary gates for quantum computation,” *Physical Review A* **52**, 3457–3467 (1995).
- [7] Michael A. Nielsen and Isaac L. Chuang, “Quantum Computation and Quantum Information,” ISBN 978-1-107-00217-3, Cambridge University Press, New York (2010) .
- [8] Vivek V. Shende, Stephen S. Bullock, and Igor L. Markov, “Synthesis of Quantum-Logic Circuits,” *IEEE Transactions on Computer-Aided Design of Integrated Circuits and Systems* **25**(6), 1000-1010
- [9] Emanuel Malvetti, Raban Iten, and Roger Colbeck, “Quantum circuits for sparse isometries,” *Quantum* **5**, 412 (2021).
- [10] J.-H. Bae, Paul M. Alsing, Doyeol Ahn, and Warner A. Miller, “Quantum circuit optimization using quantum Karnaugh map,” *Scientific reports* **10**(1), 15651 (2020).
- [11] Timothee Goubault De Brugiere, Marc Baboulin, Benoît Valiron, Simon Martiel,

and Cyril Allouche, “Reducing the depth of linear reversible quantum circuits,” IEEE Transactions on Quantum Engineering **2**, 3102422 (2021).

[12] Daniele Cuomo, Marcello Caleffi, Kevin Krsulich, Filippo Tramonto, Gabriele Agliardi, Enrico Prati, and Angela Sara Cacciapuoti, “Optimized Compiler for Distributed Quantum Computing,” ACM Transactions on Quantum Computing **4**(2), 15 1-29 (2023).

[13] Mehdi Saeedi and Massoud Pedram, “Linear-depth quantum circuits for n-qubit Toffoli gates with no ancilla,” Physical Review A **87**(6), 062318 (2013).

[14] Dmitri Maslov, “Advantages of using relative-phase Toffoli gates with an application to multiple control Toffoli optimization,” Physical Review A **93**(2), 022311 (2016).

[15] Young-Min Jun and In-Chan Choi, “Optimal Multi-Bit Toffoli Gate Synthesis,” IEEE Access **11**, 27342-27351 (2023).

[16] Adenilton J. da Silva and Daniel K. Park, “Linear-depth quantum circuits for multiqubit controlled gates,” Physical Review A **106**(4), 042602 (2022).

[17] Rafaella Vale, Thiago Melo D. Azevedo, Ismael C. S. Araújo, Israel F. Araujo, and Adenilton J. da Silva, “Circuit Decomposition of Multicontrolled Special Unitary Single-Qubit Gates,” IEEE Transactions on Computer-Aided Design of Integrated Circuits and Systems **43**(3), 802-811 (2023).

[18] Jefferson D. S. Silva , Thiago Melo D. Azevedo , Israel F. Araujo , Adenilton J. da Silva, “Linear decomposition of approximate multi-controlled single qubit gates,” arxiv.org/abs/2310.14974 (2023-10-23).

[19] Yong He, Ming-Xing Luo, E. Zhang, Hong-Ke Wang, and Xiao-Feng Wang, “Decompositions of n-qubit Toffoli Gates with Linear Circuit Complexity,” International Journal of Theoretical Physics **56**, 2350-2361 (2017).

[20] Stefan Balaucă and Andreea Arusoaiă, “Efficient Constructions for Simulating Multi Controlled Quantum Gates,” Computational Science - ICCS 2022, Springer International Publishing, Cham, **13353**, 179-194 (2022).

[21] Thomas G. Draper, “Addition on a Quantum Computer,” arxiv.org/abs/quant-ph/0008033 (2000-08-07).

[22] Vladimir V. Arsovski, “Implementing multi-controlled X gates using the quantum Fourier transform,” arxiv.org/abs/2407.18024, Submitted to a peer-reviewed journal (06-03-2024).

[23] Adriano Barenco, Artur Ekert, Kalle-Antti Suominen, and Päivi Törmä, “Approximate quantum Fourier transform and decoherence,” Phys. Rev. A **54**, 139-146 (1996).

- [24] Dimitri Maslov, “Linear depth stabilizer and quantum Fourier transformation circuits with no auxiliary qubits in finite-neighbor quantum architectures,” Phys. Rev. A **76**, 052310-1–7 (2007).
- [25] Qiskit

#### ACKNOWLEDGMENTS

This work was financially supported by the Ministry of Science, Technological Development and Innovation of the Republic of Serbia under contract number: 451-03-65/2024-03/200103.